HHS Public Access

Author manuscript

Brain Imaging Behav. Author manuscript; available in PMC 2022 August 01.

Published in final edited form as:

Brain Imaging Behav. 2021 August ; 15(4): 2051–2060. doi:10.1007/s11682-020-00399-z.

High-resolution functional connectivity of the default mode network in young adults with Down Syndrome

Katherine A. Koenig[1], **Lynn M. Bekris**[2], **Stephen Ruedrich**[3], **Grace E. Weber**[2], **Maria Khrestian**[2], **Se-Hong Oh**[1,4], **Sanghoon Kim**[1], **Z. Irene Wang**[5], **James B. Leverenz**[6]

[1]Imaging Sciences, Imaging Institute, Cleveland Clinic, Cleveland, OH, USA

[2]Genomic Medicine Institute, Cleveland Clinic, Cleveland, OH, USA

[3]Department of Psychiatry, University Hospitals, Cleveland, OH, USA

[4]Department of Biomedical Engineering, Hankuk University of Foreign Studies, Yongin, Republic of Korea

[5]Epilepsy Center, Neurological Institute, Cleveland Clinic, Cleveland, OH, USA

[6]Lou Ruvo Center for Brain Health, Neurological Institute, Cleveland Clinic, Cleveland, OH, USA

Abstract

Studies of resting-state functional connectivity MRI in Alzheimer's disease suggest that disease stage plays a role in functional changes of the default mode network. Individuals with the genetic disorder Down syndrome show an increased incidence of early-onset Alzheimer's-type dementia, along with early and nearly universal neuropathologic changes of Alzheimer's disease. The present study examined high-resolution functional connectivity of the default mode network in 11 young adults with Down syndrome that showed no measurable symptoms of dementia and 11 age- and sex-matched neurotypical controls. We focused on within-network connectivity of the default mode network, measured from both anterior and posterior aspects of the cingulate cortex. Sixty-eight percent of connections to the posterior cingulate and 26% to the anterior cingulate showed reduced strength in the group with Down syndrome ($p < 0.01$). The Down syndrome

Corresponding author: Katherine A. Koenig, Ph.D., Imaging Sciences, Imaging Institute, 9500 Euclid Ave / U15, Cleveland, OH 44195, koenigk@ccf.org, Phone: 216-445-9834.

Author Contributions

Author contributions included conception and study design (KAK, SR, JBL), methodological development (S-HO, SK), data collection or acquisition (KAK, SR, S-HO, SK, ZIW, JBL), statistical analysis (KAK, LMB, GEW, MK), interpretation of results (KAK, LMB, GEW, JBL), drafting the manuscript work or revising it critically for important intellectual content (KAK, LMB, SR, GEW, JBL) and approval of final version to be published and agreement to be accountable for the integrity and accuracy of all aspects of the work (All authors).

Compliance with Ethical Standards

All data was collected under a Cleveland Clinic Institutional Review Board-approved protocol. All participants provided written informed consent prior to any study procedures.

Conflict of Interest

None of the authors have a conflict of interest to declare.

group showed increased connectivity strength from the anterior cingulate to the bilateral inferior frontal gyri and right putamen ($p < 0.005$). In an exploratory analysis, connectivity in the group with Down syndrome showed regional relationships to plasma measures of inflammatory markers and t-tau. In non-demented adults with Down syndrome, functional connectivity within the default mode network may be analogous to changes reported in preclinical Alzheimer's disease, and warrants further investigation as a measure of dementia risk.

Keywords

Down syndrome; functional MRI; Alzheimer's disease; dementia; default mode network

Introduction

Down syndrome (DS) is a common genetic cause of developmental disability, and is associated with an increased incidence of early onset dementia and neuropathologic changes of Alzheimer's disease (AD) (Visser et al., 1997). The triplicate of chromosome 21 in DS results in an additional copy of the amyloid precursor protein (*APP*) gene, which is responsible for the synthesis of beta-amyloid (Aβ) protein that is found in the senile plaques of AD. The overexpression of APP is thought to lead to increased Aβ in the brain of those with DS (Teller et al., 1996).

Multiple studies have shown similarities in the relation of neuroimaging measures to dementia in DS with those found in the non-DS AD population (Beacher et al., 2009; Lamar et al., 2011; Prasher et al., 2003), though it has proven difficult to disambiguate changes resulting from AD-related pathology, aging, and developmental disability (Kesslak et al., 1994; Teipel et al., 2004). Even in the absence of measurable cognitive decline, extracellular Aβ deposition is consistently reported by the fourth decade of life in those with DS (Mann & Esiri, 1989; Sabbagh et al., 2015), and has been reported in younger individuals (Lemere et al., 1996; Leverenz & Raskind, 1998). In preclinical AD, Aβ accumulation has been found in the precuneus, posterior cingulate, and medial orbitofrontal cortex (Palmqvist et al., 2017), regions that are part of a functional brain network known as the default mode network (DMN). In healthy controls, regions within the DMN show strong functional connections while participants are at rest, and has been implicated in processes related to a "resting-state," such as self-generated thought (Andrews-Hanna et al., 2014; Horn et al., 2014). Decreases in the strength of these connections have been reported in preclinical AD and in those at genetic risk for AD (Palmqvist et al., 2017; Zhang et al., 2010), although work investigating DMN sub-networks suggests that early decreases are driven by posterior regions of the network (Damoiseaux et al., 2012).

This study used high-resolution fMRI to assess resting-state functional connectivity (rsfMRI) of the DMN in a sample of non-demented adults with DS. To differentiate the posterior and anterior aspects of the DMN, a seed-based analysis focused on the posterior (PCC) and anterior (ACC) cingulate cortices. We hypothesized that individuals with DS would show a similar pattern to that reported in clinical and preclinical AD - decreased connectivity within the DMN, driven by posterior aspects of the network. We recently

reported evidence of an altered immune profile in DS, including increased levels of plasma inflammatory markers and the soluble cleavage product of triggering receptor expressed in myeloid cells-2 (sTREM2) (Weber et al., 2020). Here, we report results of an exploratory analysis in the DS group, relating rsfMRI to cognitive performance and to plasma measures of sTREM2, inflammatory cytokines, $A\beta_{1–42}$, $A\beta_{1–40}$, and total tau (t-tau).

Methods

Participants

Participants included 13 adults with a medical diagnosis of trisomy 21 (mean age 29.7, range 26–35, 8 males). Prior to data analysis, an age- and sex-matched control group was selected from neurotypical, healthy controls that were scanned during roughly the same time period, on the same scanner, using identical scanning protocols. Exclusion criteria for all participants included: 1. History of major psychiatric disorder 2. Neurologic history such as head injury, stroke, or epilepsy 3. The inability to complete study procedures due to physical or cognitive limitations 4. Confirmed clinical symptoms of dementia 5. MRI-specific exclusion criteria. For each participant, data was collected in a single session after providing written informed consent.

Data Acquisition

Behavioral testing—To minimize the chance that a participant may be showing subtle signs of undiagnosed dementia, each participant with DS underwent a comprehensive clinical assessment with a psychiatrist specializing in developmental disabilities. This assessment included medical history, a psychiatric diagnostic interview with participant and caregiver, and mental status examination. Participant caregivers also completed the Dementia Screening Questionnaire for Individuals with Intellectual Disabilities (DSQIID) (Deb et al., 2007) and the Dementia Questionnaire for People with Learning Disabilities (DLD) (Evenhuis, 1996).

Cognitive function was assessed in those with DS using the Down’s syndrome Attention, Memory and Executive function battery (DAMES) (Margallo-Lana, Moore, et al., 2007), resulting in total score and composite scores in the domains of attention, memory, and executive function, and the short-form Prudhoe Cognitive Function Test (PCFT) (Margallo-Lana, Moore, et al., 2003), resulting in total score.

Biological specimens—Biological specimens were only available for individuals with DS. Clinical laboratory testing was used to rule out treatable causes of cognitive impairment, including complete blood panel with differential, CMP, folate, vitamin B12, and TSH. To quantify $A\beta_{1–40}$, $A\beta_{1–42}$, and t-tau, plasma extracted from blood was diluted 1:5 and measured using MILLIPLEX MAP® multiplex kits and analyzed using a Luminex 200 3.1 xPONENT System (Luminex xMAP technology; EMD Millipore, Chicago, IL, USA) following the manufacturer’s instructions (Shi et al., 2011). The details of sTREM2 and inflammatory cytokine measurement in this sample are previously described (Weber et al., 2020).

MR imaging—All participants were scanned on a Siemens 7T Magnetom with SC72 gradient (Siemens Medical Solutions, Erlangen) using a head-only CP transmit and 32-channel phased-array receive coil (Nova Medical, Wilmington). Scans included:

1. Whole-brain coverage, T1-weighted anatomical scan: MP2RAGE (Marques et al., 2010), 0.75mm^3 isotropic voxels, scan time 10 minutes.
2. Resting state functional connectivity scan: 132 repetitions of 81 axial slices, voxel size 0.75×0.75×1.5mm^3, TE/TR=21ms/2800ms, matrix 160×160, FOV 210×210mm^2, receive bandwidth = 1562 Hz/pixel, scan time 7 minutes.

Data Analysis

Volumetric analysis—Total white matter (WM), total and subcortical grey matter (GM), and ventricular volumes were estimated using the MP2RAGE in Freesurfer 6.0 (Freesurfer, 2017) and corrected for intracranial volume. T-tests were used to assess group differences and the false discovery rate (FDR) was used to adjust for multiple comparisons.

Pre-processing of functional data—The first 4 volumes of the functional time series were removed. Cardiac and respiratory signals were measured during scanning and regressed out at the voxel level using RETROICOR (Glover et al., 2000). Volumetric and slice-wise motion was retrospectively corrected using SLOMOCO (Beall & Lowe, 2014), including regression of volume-wise residual motion estimates. Residual motion estimates were compared between groups. The data were spatially filtered using a 2mm filter (Cox, 1996), fluctuations above 0.08 Hz were removed, and the data was detrended. The anatomical scan was aligned to the functional volume using the AFNI program align_epi_anat.py (Saad et al., 2009) and transformed to Talairach space using nonlinear warping (Avants et al., 2008).

Seed selection and rsfMRI analysis—Seed selection took place in native rsfMRI space for each participant. The PCC seed was identified by the use of a 6-mm sphere, placed according to previously identified Talairach coordinates (Greicius et al., 2003), and transferred to rsfMRI space. A voxel-wise search was conducted within the PCC region of interest (ROI) to identify the voxel with the highest correlation to other DMN regions as defined in the Yeo et al. (2011) 7 network parcellation (Lowe et al., 2014; Yeo et al., 2011). A nine-voxel in-plane ROI was centered at that voxel, and served as the PCC seed. The ACC seed comprised a nine-voxel region centered at the voxel within the left ACC with the highest correlation to the PCC seed. Separate rsfMRI maps were created for the PCC and ACC by correlating the average time series of each seed with the time series of each voxel in brain tissue. To account for individual differences in global signal, each correlation was converted to a Student's t-score, and the whole-brain distribution was normalized to unit variance and zero mean (Lowe et al., 1998).

Individual correlation maps were transferred to Talairach space and averaged by group. For each seed, group maps were thresholded (single voxel threshold $p < 0.001$, whole brain probability $p < 0.05$ with a cluster size = 200) and added to create a mask of all regions showing significant connectivity to that seed. Regions that included multiple significant

peaks were eroded to create smaller ROIs centered on each peak. PCC and ACC ROI masks were transformed to native space for each participant, and mean connectivity was calculated for each ROI. Student's t-tests were used to assess group differences. The FDR adjustment was applied separately for the PCC and ACC ROI sets. In the DS group, linear correlations examined the relationship of mean connectivity of each ROI to cognitive scores and plasma measures. The FDR adjustment was applied separately for the entire set of correlations associated with each seed region.

Results

Participants

No participants were excluded for potential signs of dementia. After MRI image pre-processing, rsfMRI datasets were inspected for visual signs of motion corruption, including assessments of head movement during the time series and artifacts in correlation maps such as rapid pattern changes from slice to slice and correlation in the ventricles. Two participants with DS had evidence of motion-corrupted data and were excluded from further analysis. Prior to further data analysis, the remaining 11 participants (mean age 29.4, range 26–35, 7 males) were age- and sex-matched with 11 neurotypical controls (mean age 29.8, range 24–36, 7 males).

Biological specimens

Values of inflammatory cytokines, sTREM2, $A\beta_{1–42}$, $A\beta_{1–40}$, and t-tau were $\log_{10}$ transformed for comparison. One participant was excluded from the correlation analysis because all measured values were outside of the detectable range of the assays. Seven measures had one value that was out of range, distributed across four participants: Flt-3L, IFNα2, MCP-3, IL-12P40, IL-4, IL-7, TNFβ.

Volumetric analysis

Intracranial volume was smaller in those with DS (p = 0.0251), but there were no group differences in corrected cerebral WM, cortical or subcortical GM, or ventricular volumes.

RsfMRI of the DMN

The residual motion estimates from SLOMOCO were compared between groups. Despite removal of 2 participants with obvious motion artifacts, the DS group showed increased residual mean (DS = 0.50mm ± 0.15, control = 0.05mm ± 0.04, $p = 5.1 \times 10^{-9}$) and maximum (DS = 2.5mm ± 1.2, control = 0.20 ± 0.17, $p = 6.2 \times 10^{-6}$) motion. Although these residual motion estimates were included as regressors in data pre-processing, group differences in motion characteristics may impact our results.

Figure 1 shows average connectivity to the left PCC in: A1. the group with DS and A2. controls and to the left ACC in: B1. the group with DS and B2. controls ($p < 0.001$, cluster size = 200). Table 1 details regions that were significantly connected to each seed in either group. Both seeds showed extensive connections to regions typically reported as belonging to the DMN. Regions specific to each seed included additional frontal lobe and subcortical

GM connections to the ACC, and hippocampal, parahippocampal gyrus, and precuneus connections to the PCC.

Compared to controls, the DS group showed widespread changes in connectivity to both seeds (Table 1). In DS, strength was reduced in 17 of 25 ROIs (68%) connected to the PCC and 13 of 34 ROIs (26%) connected to the ACC. Three of 34 ROIs (9%) showed increased strength of connection to the ACC, including the bilateral inferior frontal gyri and right putamen. Non-significant increases were also observed in the left caudate, right middle frontal gyrus, left anterior insula, and left putamen. No regions showed increased connectivity to the PCC in the DS group.

Correlation analysis

Age was not related to connectivity in the DS group. The only significant relationship to cognitive scores was a negative correlation between the DAMES memory score and connectivity of the ACC to the left ($r = -0.683$, $p = 0.0206$) and right medial frontal gyri ($r = -0.721$, $p = 0.0122$), although only the right survived FDR correction.

Table 2 shows correlation coefficients for rsfMRI regions that showed a significant relationship to plasma measures. $A\beta_{1–40}$ and $A\beta_{1–42}$ were not significantly related to connectivity. Only one region showed a negative relationship between connectivity and inflammatory cytokines, that of the PCC to the left inferior temporal gyrus (BA 20; Figure 2A). Inflammatory cytokines were positively related to connectivity between the PCC and the left inferior frontal gyrus (BA 47) and between the ACC and the left and right angular gyri, right inferior frontal gyrus (BA 47), and the left thalamus. ACC-left angular gyrus connectivity showed a positive relationship to sTREM2 levels (Figure 2B), and ACC-right angular gyrus connectivity was related to T-tau ($r = 0.754$, $p = 0.0117$).

Discussion

Using high-resolution functional imaging, we assessed within-network connectivity of the posterior and anterior DMN in DS. This work leveraged gains in signal-to-noise ratio and increased spatial resolution achievable using high-field MRI by using small connectivity seeds that are representative of the functional network in question, and by taking functional measurements from native space, minimizing the impact of partial volume effects and errors due to image registration.

Reduced DMN connectivity has been reported in clinical and preclinical AD (Palmqvist et al., 2017; Wu et al., 2011; Zhang et al., 2010) and in cognitively normal individuals with increased amyloid burden (Hedden et al., 2009). There are also reports of regional connectivity increases in early AD and in populations at genetic risk (Machulda MM et al., 2011; Patel et al., 2013), and evidence that anterior and posterior sub-networks of the DMN are differentially impacted (Damoiseaux et al., 2012; Westlye et al., 2011). Young adults with DS may show no clinical symptoms of dementia, but likely have neuropathologic changes associated with AD (Leverenz & Raskind, 1998). We hypothesized that connectivity would be decreased in this group, primarily driven by the posterior aspect of the DMN.

Early studies of rsfMRI in DS focused on between-network connectivity, showing that, compared to controls, those with DS have increased connection strength between functional networks (Anderson et al., 2013; Vega et al., 2015). In a seed-based analysis of DMN connectivity, Wilson et al. (2019) compared controls to participants with DS categorized as amyloid positive or negative using PiB PET (Wilson et al., 2019). In the younger amyloid-negative group, connectivity was decreased between the left medial frontal gyrus and the ACC. The older amyloid-positive group showed more widespread reductions, including to posterior regions of the DMN. Our findings are similar to the changes seen in the amyloid-positive group, despite our younger sample that is less likely to have positive PiB scans (LeVine et al., 2017). In a sample of similar age to our own, Pujol et al. (2015) found globally decreased connectivity of the PCC, posterior insula, dorsal prefrontal cortex, and dorsal ACC in DS. The ventral ACC showed an increase in global connectivity, including increased connectivity to the anterior insula, in line with the current findings (Pujol et al., 2015). Our results are notable in that, although the DS group showed decreased DMN connectivity overall, group differences reflected an anterior/posterior differentiation that has been previously reported in those at genetic risk of AD (Patel et al., 2013). Longitudinal imaging in a larger sample is required to clarify connectivity differences that are indicators of dementia risk, associated with DS, or that interact with age or other factors.

The variability of Aβ deposition within DS, both across age and in relation to dementia onset, suggests that other factors are related to the onset of AD (Leverenz & Raskind, 1998; Rafii et al., 2017). We found no relationship between measures of Aβ and connectivity, although given previous reports of equivalent plasma Aβ measures in asymptomatic vs. prodromal AD adults with DS, this is not entirely unexpected (Fortea et al., 2018). Measures of immune response and peripheral inflammation are elevated in DS (Iulita et al., 2016; Weber et al., 2020; Zhang et al., 2017), including sTREM2 (Raha-Chowdhury et al., 2019; Weber et al., 2020), which is associated with Aβ and cognitive decline in the non-DS population. Our recent report of an altered relationship between sTREM2 and inflammation in DS (Weber et al., 2020) led to an exploratory analysis of the relationship between connectivity and these measures. Inflammatory cytokine levels were negatively related to the strength of connectivity from the PCC to the anterior aspect of the left ITG, a region that is related to semantic processing (Binney et al., 2010) and shows AD-related synaptic loss (Scheff et al., 2011). Notably, this relationship was significant for markers such as TNFα and IL-6, which multiple reports have described as increased in DS (Iulita et al., 2016; Sullivan et al., 2017; Weber et al., 2020). Interestingly, sTREM2 and a generally non-overlapping set of markers were positively related to connectivity of the ACC. Without additional work, the meaning of these variable relationships is unclear, but they suggest that altered immune response in DS should be considered in efforts to develop dementia-related biomarkers.

Although these results are intriguing, they must be interpreted with caution. This is a small sample, and the findings require replication. Our use of plasma measures of amyloid and tau is not ideal, although more preferable measures taken from CSF were not available. A major limitation of our study, and of all published functional MRI studies in DS, is that of head motion. Head motion can result in changes in connectivity (Van Dijk et al., 2012), and group differences in motion are of particular concern. Our motion correction method

accounts for both volumetric and slice-wise motion effects, and volumetric estimates of residual motion were included as regressors. The relatively consistent connectivity patterns shown by two spatially distinct seed regions with the DMN, the finding of both increased and decreased regions of connectivity in the DS group, and the fact our findings are in agreement with previous work (Pujol et al., 2015) gives us a measure of confidence in our results. Regardless, the impact of motion on our results cannot be discounted.

Conclusions

In a sample of young adults with DS and no symptoms of dementia, we find decreased connectivity strength within the DMN. We investigated anterior/posterior DMN differentiation and found, first, a greater percentage of weakened connections to the PCC, and second, locally increased connectivity to the ACC. These findings are similar to those reported in preclinical AD, and indicate that early functional changes in DS may be related to AD pathophysiology and have to potential to function as predictors of dementia risk.

Acknowledgements

The authors thank Tobias Kober and Thomas Benner of Siemens Healthineers for use of WIP 944 and WIP 770B.

Funding Sources

This work was supported by Alzheimer’s Association (2016-NIRG-395687). As a trainee of the research education component of the Cleveland Alzheimer’s Disease Research Center, the work of K. Koenig was in part supported by the National Institute on Aging (P30 AG062428 01).

Abbreviations

ACC	anterior cingulate cortex
AD	Alzheimer’s disease
APP	amyloid precursor protein
Aβ	beta-amyloid
DAMES	Down’s syndrome Attention, Memory and Executive function battery
DLD	Dementia Questionnaire for People with Learning Disabilities
DMN	default mode network
DS	Down Syndrome
DSQIID	Dementia Screening Questionnaire for Individuals with Intellectual Disabilities
FDR	false discovery rate
GM	grey matter
ITG	inferior temporal gyrus

PCC	posterior cingulate cortex
PCFT	Prudhoe Cognitive Function Test
ROI	region of interest
rsfMRI	resting-state functional MRI connectivity
sTREM2	soluble cleavage product of triggering receptor expressed in myeloid cells-2
WM	white matter

References

Anderson JS, Nielsen JA, Ferguson MA, Burback MC, Cox ET, Dai L, Gerig G, Edgin JO, & Korenberg JR (2013). Abnormal brain synchrony in Down Syndrome. NeuroImage: Clinical, 2, 703–715. [PubMed: 24179822]

Andrews-Hanna JR, Smallwood J, & Spreng RN (2014). The default network and self-generated thought: Component processes, dynamic control, and clinical relevance. Annals of the New York Academy of Sciences, 1316(29), 52.

Avants BB, Epstein CL, Grossman M, & Gee JC (2008). Symmetric Diffeomorphic Image Registration with Cross-correlation: Evaluating Automated Labeling of Elderly and Neurodegenerative Brain. . Med Image Anal, 12(1), 26–41. [PubMed: 17659998]

Beacher F, Daly E, Simmons A, Prasher V, Morris R, Robinson C, Lovestone S, Murphy K, & Murphy DGM (2009). Alzheimer's disease and Down's syndrome: an in vivo MRI study. Psychological Medicine, 39, 675–684. [PubMed: 18667098]

Beall EB, & Lowe MJ (2014). SimPACE: generating simulated motion corrupted BOLD data with synthetic-navigated acquisition for the development and evaluation of SLOMOCO: a new, highly effective slicewise motion correction. Neuroimage, 101, 21–34. [PubMed: 24969568]

Binney RJ, Embleton KV, Jefferies E, Parker GJ, & Ralph MA (2010). The ventral and inferolateral aspects of the anterior temporal lobe are crucial in semantic memory: evidence from a novel direct comparison of distortion-corrected fMRI, rTMS, and semantic dementia. Cereb Cortex, 20(11), 2728–2738. [PubMed: 20190005]

Cox R (1996). AFNI: Software for analysis and visualization of functional magnetic resonance neuroimages. Computers and Biomedical Research, 29, 162–173. [PubMed: 8812068]

Damoiseaux JS, Prater K, Miller BL, & Greicius MD (2012). Functional connectivity tracks clinical deterioration in Alzheimer's disease. Neurobiol Aging, 33(4), 828.e819–828.e830.

Deb S, Hare M, Prior L, & Bhaumik S (2007). Dementia screening questionnaire for individuals with intellectual disabilities. Br J Psychiatry, 190, 440–444. [PubMed: 17470960]

Evenhuis HM (1996). Further evaluation of the Dementia Questionnaire for Persons with Mental Retardation. J Intellectual Disabilities Res, 40(4), 369–373.

Fortea J, Carmona-Iragui M, Benejam B, Fernández S, Videla L, Barroeta I, Alcolea D, Pegueroles J, Muñoz L, Belbin O, de Leon MJ, Maceski AM, Hirtz C, Clarimón J, Videla S, Delaby C, Lehmann S, Blesa R, & Lleó A (2018). Plasma and CSF biomarkers for the diagnosis of Alzheimer's disease in adults with Down syndrome: a cross-sectional study. Lancet Neurol, 17(10), 860–869. [PubMed: 30172624]

Freesurfer. (2017). version 6.0.0http://surfer.nmr.mgh.harvard.edu/.

Glover GH, Li T, & Ress D (2000). Image-Based Method for Retrospective Correction of Physiological Motion Effects in fMRI: RETROICOR. Magnetic Resonance in Medicine, 44, 162–167. [PubMed: 10893535]

Greicius MD, Krasnow B, Reiss AL, & Menon V (2003). Functional connectivity in the resting brain: A network analysis of the default mode hypothesis. PNAS, 100(1), 253–258. [PubMed: 12506194]

Hedden T, Van Dijk KRA, Becker JA, Mehta A, Sperling RA, Johnson KA, & Buckner RL (2009). Disruption of Functional Connectivity in Clinically Normal Older Adults Harboring Amyloid Burden. J Neurocience, 29(40), 12686–12694.

Horn A, Ostwald D, Reisert M, & Blankenburg F (2014). The structural-functional connectome and the default mode network of the human brain. Neuroimage, 102(1), 142–151. [PubMed: 24099851]

Iulita MF, Ower A, Barone C, Pentz R, Gubert P, Romano C, Cantarella RA, Elia F, Buono S, Recupero M, Romano C, Castellano S, Bosco P, Di Nuovo S, Drago F, Caraci F, & Cuello AC (2016). An inflammatory and trophic disconnect biomarker profile revealed in Down syndrome plasma: Relation to cognitive decline and longitudinal evaluation. Alzheimers Dementia, 12(11), 1132–1148.

Kesslak JP, Nagata SF, Lott IT, & Nalcioglu O (1994). MRI analysis of age-related changes in the brains of individuals with DS. Neurology, 44, 1039–1045. [PubMed: 8208396]

Lamar M, Foy CML, Beacher F, Daly E, Poppe M, Archer N, Prasher V, Murphy KC, Morris RG, Simmons A, Lovestone S, & Murphy DGM (2011). Down syndrome with and without dementia: An in vivo proton Magnetic Resonance Spectroscopy study with implications for Alzheimer's disease. Neuroimage, 57, 63–68. [PubMed: 21504795]

Lemere CA, Blusztajn JK, Yamaguchi H, Wisniewski T, Saido TC, & Selkoe DJ (1996). Sequence of deposition of heterogeneous amyloid beta-peptides and APO E in Down syndrome: implications for initial events in amyloid plaque formation. Neurobiology of Disease, 3(1), 16–32. [PubMed: 9173910]

Leverenz JB, & Raskind MA (1998). Early amyloid deposition in the medial temporal lobe of young Down syndrome patients: a regional quantitative analysis. Exp Neurol, 150(2), 296–304. [PubMed: 9527899]

LeVine H, Spielmann PH, Matveev S, Cauvi FM, Murphy MP, Beckett TL, McCarty K, Lott IT, Doran E, Schmitt F, & Head E (2017). Down syndrome: Age-dependence of PiB binding in postmortem frontal cortex across the lifespan. Neurobiol Aging, 54, 163–169. [PubMed: 28385551]

Lowe M, Koenig K, Beall E, Sakaie K, Stone L, Bermel R, & Phillips M (2014). Anatomic connectivity assessed using pathway radial diffusivity is related to functional connectivity in monosynaptic pathways. Brain Connectivity, 4(7), 558–565. [PubMed: 25117651]

Lowe MJ, Mock BJ, & Sorenson JA (1998). Functional Connectivity in Single and Multislice Echoplanar Imaging Using Resting-State Fluctuations. Neuroimage, 7(2), 119–132. [PubMed: 9558644]

Machulda MM, Jones DT, Vemuri P, McDade E, Avula R, Przybelski S, Boeve BF, Knopman DS, Petersen RC, & Jack CR (2011). Effect of APOE ε4 Status on Intrinsic Network Connectivity in Cognitively Normal Elderly Subjects. Arch Neurology, 68(9), 1131–1136.

Mann DM, & Esiri MM (1989). The pattern of acquisition of plaques and tangles in the brains of patients under 50 years of age with Down's syndrome. J Neurol Sci., 89(2–3), 169–179. [PubMed: 2522541]

Margallo-Lana M, Moore PB, Kay DWKet al. (2007). 15-year follow up of 92 hospitalised adults with Down's Syndrome: Relationship of cognitive decline to neurofibrillary tangle count. J Intellect Disabil Res 51: 463–477. [PubMed: 17493029]

Margallo-Lana ML, Moore PB, Tyrer SP, Dawson H, Jenkins K, & Kay DW (2003). The Prudhoe Cognitive Function Test, a scale to assess cognitive function in adults with Down's syndrome: inter-rater and test-retest reliability. Journal Of Intellectual Disability Research, 47(6), 488–492. [PubMed: 12919200]

Marques JP, Kober T, Krueger G, van der Zwaag W, Van de Moortele PF, & Gruetter R (2010). MP2RAGE, a self bias-field corrected sequence for improved segmentation and T1-mapping at high field. Neuroimage, 49, 1271–1281. [PubMed: 19819338]

Palmqvist S, Schöll M, Strandberg O, Mattsson N, Stomrud E, Zetterberg H, Blennow K, Landau S, Jagust W, & Hansson O (2017). Earliest accumulation of β-amyloid occurs within the default-mode network and concurrently affects brain connectivity. Nature Communications, 8, 1214.

Patel KT, Stevens MC, Pearlson GD, Winkler AM, Hawkins KA, Skudlarski P, & Bauer LO (2013). Default mode network activity and white matter integrity in healthy middle-aged ApoE4 carriers. Brain Imaging and Behavior, 7(1), 60–67. [PubMed: 23011382]

Prasher V, Cumella S, Natarajan K, Rolfe E, Shah S, & Haque MS (2003). Magnetic resonance imaging, Down's syndrome and Alzheimer's disease : research and clinical implications. Journal of Intellectual Disabilities Research, 47, 90–100.

Pujol J, del Hoyo L, Blanco-Hinojo L, de Sola S, Macià D, Martínez-Vilavella G, Amor M, Deus J, Rodríguez J, Farré M, Dierssen M, & de la Torre R (2015). Anomalous brain functional connectivity contributing to poor adaptive behavior in Down syndrome. Cortex, 64, 148–156. [PubMed: 25461715]

Rafii MS, Lukic AS, Andrews RD, Brewer J, Rissman RA, Strother SC, Wernick MN, Pennington C, Mobley WC, Ness S, Matthews DC, & Initiative, D. S. B. I. a. t. A. s. D. N. (2017). PET Imaging of Tau Pathology and Relationship to Amyloid, Longitudinal MRI, and Cognitive Change in Down Syndrome: Results from the Down Syndrome Biomarker Initiative (DSBI). J Alzheimers Dis, 60(2), 439–450. [PubMed: 28946567]

Raha-Chowdhury R, Henderson JW, Raha AA, Vuono R, Bickerton A, Jones E, Fincham R, Allinson K, Holland A, & Zaman SH (2019). Choroid Plexus Acts as Gatekeeper for TREM2, Abnormal Accumulation of ApoE, and Fibrillary Tau in Alzheimer's Disease and in Down Syndrome Dementia. J Alzheimers Dis, 69(1), 91–109. [PubMed: 30909239]

Saad ZS, Glen DR, Chen G, Beauchamp MS, Desai R, & Cox RW (2009). A new method for improving functional-to-structural alignment using local Pearson correlation. Neuroimage, 44, 839–848. [PubMed: 18976717]

Sabbagh MN, Chen K, Rogers J, Fleisher AS, Liebsack C, Bandy D, Belden C, Protas H, Thiyyagura P, Liu X, Roontiva A, Luo J, Jacobson S, Malek-Ahmadi M, Powell J, & Reiman EM (2015). Florbetapir PET, FDG PET, and MRI in Down syndrome individuals with and without Alzheimer's dementia. Alzheimers Dementia, 11(8), 994–1004.

Scheff SW, Price DA, Schmitt FA, Scheff MA, & Mufson EJ (2011). Synaptic Loss in the Inferior Temporal Gyrus in Mild Cognitive Impairment and Alzheimer's Disease. Journal of Alzheimer's Disease, 24(3), 547–557.

Shi M, Bradner J, Hancock AM, Chung KA, Quinn JF, Peskind ER, Galasko D, Jankovic J, Zabetian CP, Kim HM, Leverenz JB, Montine TJ, Ginghina C, Kang UJ, Cain KC, Wang Y, Aasly J, Goldstein D, & Zhang J (2011). Cerebrospinal fluid biomarkers for Parkinson disease diagnosis and progression. Ann Neurol, 69(3), 570–580. 10.1002/ana.22311 [PubMed: 21400565]

Sullivan KD, Evans D, Pandey A, Hraha TH, Smith KP, Markham N, Rachubinski AL, Wolter-Warmerdam K, Hickey F, Espinosa JM, & Blumenthal T (2017). Trisomy 21 causes changes in the circulating proteome indicative of chronic autoinflammation. Scientific Reports, 7, 14818. [PubMed: 29093484]

Teipel SJ, Alexander GE, Schapiro MB, Moller HJ, Rapoport SI, & Hampel H (2004). Age-related cortical grey matter reductions in non-demented Down's sydrome adults determined by MRI with voxel-based morphometry. Brain, 127, 811–824. [PubMed: 14985261]

Teller JK, Russo C, DeBusk LM, Angelini G, Zacceo D, Dagna-Bricarelli F, Scartezzini P, Bertolini F, Mann DM, Tabaton M, & Gambetti P (1996). Presence of soluble amyloid b-peptide precedes amyloid plaque formation in Down's syndrome. Nature Medicine, 2(1), 93–95.

Van Dijk KRA, Sabuncu MR, & Buckner RL (2012). The influence of head motion on intrinsic functional connectivity MRI. Neuroimage, 59(1), 431–438. [PubMed: 21810475]

Vega JN, Hohman TJ, Pryweller JR, Dykens EM, & Thornton-Wells TA (2015). Resting-State Functional Connectivity in Individuals with Down Syndrome and Williams Syndrome Compared with Typically Developing Controls. Brain Connectivity, 5(8), 461–475. [PubMed: 25712025]

Visser FE, Aldenkamp AP, van Huffelen AC, Kuilman M, Overweg J, & van Wijk J (1997). Prospective study of the Alzheimer-type dementia in institutionalized individuals with Down syndrome. Am J of Mental Retardation, 101, 400–412.

Weber GE, Koenig KA, Khrestian M, Shao Y, Tuason ED, Gramm M, Lal D, Leverenz JB, & Bekris LM (2020). Altered Relationship between Soluble TREM2 and Inflammatory Markers in Young Adults with Down Syndrome: A Preliminary Report. Journal of Immunology. 10.4049/jimmunol.1901166

Westlye ET, Lundervold A, Rootwelt H, Lundervold AJ, & Westlye LT (2011). Increased hippocampal default mode synchronization during rest in middle-aged and elderly APOE ε4 carriers: relationships with memory performance. J Neurosci, 31(21), 7775–7783. [PubMed: 21613490]

Wilson LR, Vatansever D, Annus T, Williams GB, Hong YT, Fryer TD, Nestor PJ, Holland AJ, & Zaman SH (2019). Differential effects of Down's syndrome and Alzheimer's neuropathology on default mode connectivity. Human Brain Mapping, 40(15), 4551–4563. [PubMed: 31350817]

Wu X, Li R, Fleisher AS, Reiman EM, Guan X, Zhang Y, Chen K, & Yao L (2011). Altered default mode network connectivity in Alzheimer's disease--a resting functional MRI and Bayesian network study. Human Brain Mapping, 32(11), 1868–1881. [PubMed: 21259382]

Yeo BTT, Krienen FM, Sepulcre J, Sabuncu MR, Lashkari D, Hollinshead M, Roffman JL, Smoller JW, Zollei L, Polimeni JR, Fischl B, Liu H, & Buckner RL (2011). The organization of the human cerebral cortex estimated by intrinsic functional connectivity. J Neurophysiol, 106, 1125–1165. [PubMed: 21653723]

Zhang HY, Wang SJ, Liu B, Ma ZL, Yang M, Zhang ZJ, & Teng GJ (2010). Resting brain connectivity: changes during the progress of Alzheimer disease. Radiology, 256(2), 598–606. [PubMed: 20656843]

Zhang Y, Che M, Yuan J, Yu Y, Cao C, Qin XY, & Cheng Y (2017). Aberrations in circulating inflammatory cytokine levels in patients with Down syndrome: a meta-analysis. Oncotarget, 8(48), 84489–84496. [PubMed: 29137441]

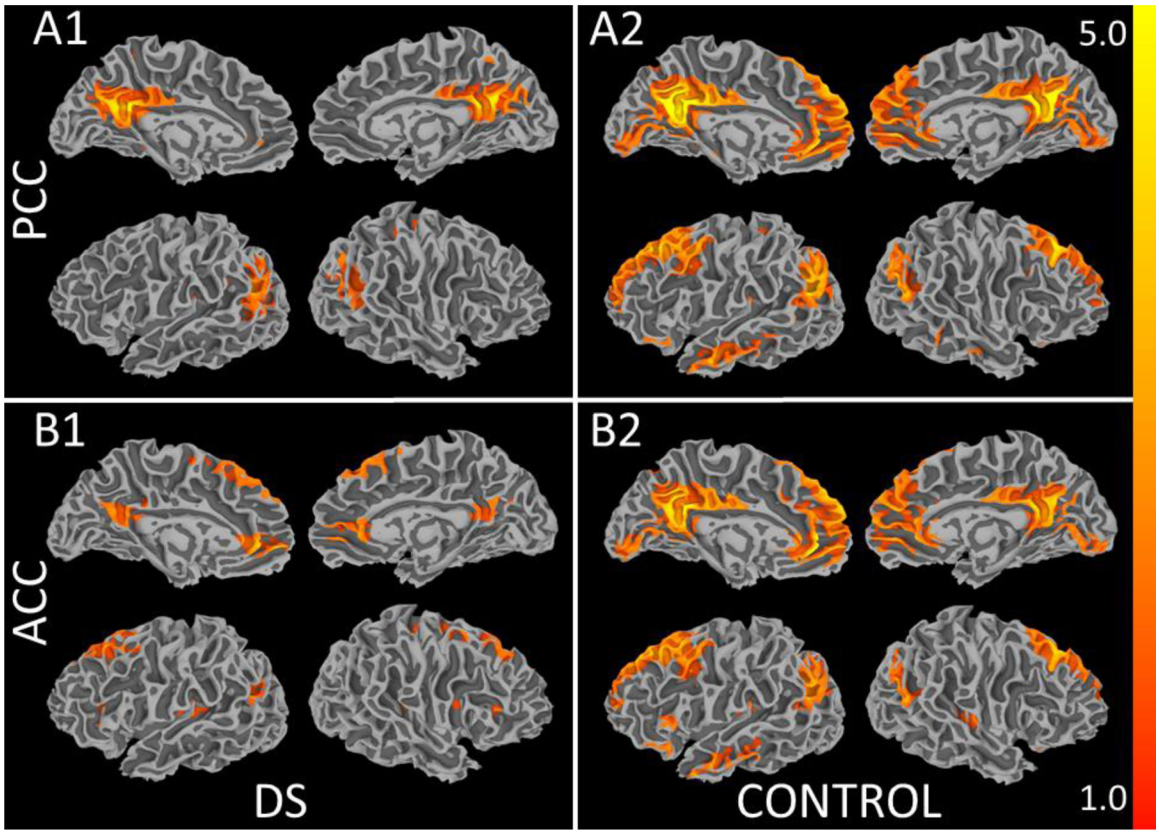

Figure 1.

Average connectivity to the left PCC in A1. the group with DS and in A2. neurotypical controls and to the left ACC in B1. the group with DS and in B2. neurotypical controls ($p < 0.001$, cluster size = 200).

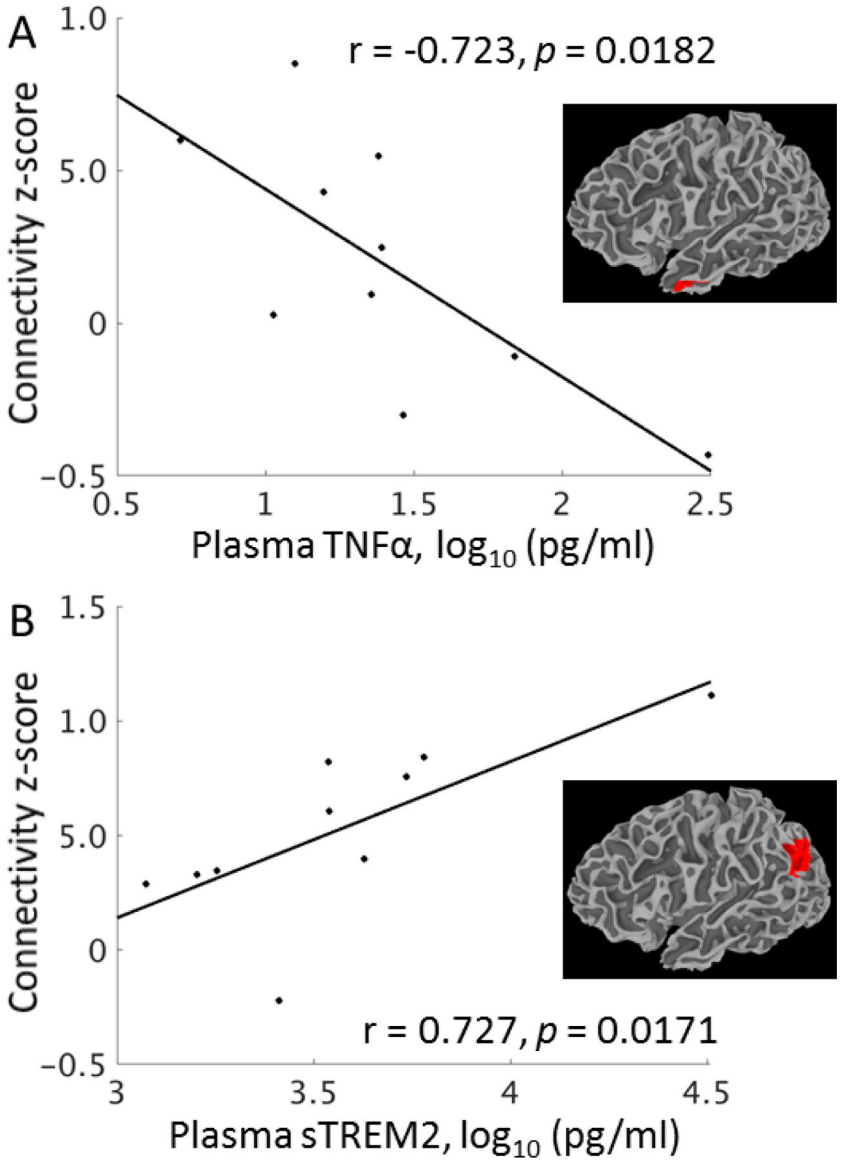

Figure 2.

The relationship of connectivity to select plasma measures in DS. A. Average connectivity from the PCC to left inferior temporal gyrus is related to TNFα, an inflammatory cytokine previously reported to be increased in DS. B. Average connectivity from the ACC to the left angular gyrus is related to sTREM2.

Table 1.

Group differences in regions showing significant connectivity to the PCC and ACC seeds.

			Talairach Coordinates			p *	
	Region	**BA**	**x**	**y**	**z**	**PCC**	**ACC**
	Both PCC and ACC						
L	superior frontal gyrus	10	−22	56	11	0.0435	0.3528
L	superior frontal gyrus	8	−20	26	47	**0.0005**	0.0432
R	superior frontal gyrus	8	25	30	45	**0.0006**	0.0439
L	middle frontal gyrus	6	−38	10	50	**0.0093**	0.3745
L	inferior frontal gyrus	47	−42	28	−10	**0.0002**	**0.0007**
R	inferior frontal gyrus	47	39	28	−12	**0.0008**	0.0260
L	medial frontal gyrus	9	−4	53	20	**7.7×10^{-6}**	**0.0001**
R	medial frontal gyrus	9	5	46	25	**0.0008**	0.0125
L	medial frontal gyrus	8	−6	45	43	**0.0020**	**0.0061**
L	insula, posterior	13	−35	−19	20	0.9018	0.2097
R	anterior cingulate	32	8	38	15	**6.9×10^{-5}**	0.0510
R	posterior cingulate	23	5	−50	19	0.1202	**0.0024**
L	angular gyrus	39	−41	−61	29	0.0263	**0.0011**
R	angular gyrus	39	52	−61	27	0.5147	0.0288
L	middle temporal gyrus	21	−56	−3	−16	**0.0012**	0.0200
R	middle temporal gyrus	21	56	−4	−19	**0.0016**	0.0582
L	inferior temporal gyrus	20	−49	7	−24	**0.0002**	**0.0015**
R	cerebellum, lobule 7		21	−81	−28	**1.6×10^{-5}**	**0.0001**
	PCC only						
L	anterior cingulate	32	−5	41	14	**6.1×10^{-5}**	
L	hippocampus		−25	−17	−10	**0.0006**	
R	hippocampus		24	−15	−14	**0.0022**	
L	parahippocampal gyrus	35	−27	−34	−11	0.0618	
L	precuneus	31	−2	−61	25	0.0747	
R	precuneus	31	6	−58	27	0.6664	
L	cerebellum, lobule 7		−34	−76	−28	**0.0081**	
	ACC only						
L	superior frontal gyrus	9	−12	48	33		**0.0020**
L	middle frontal gyrus	9	−45	17	34		0.0100
R	middle frontal gyrus	46	42	47	6		0.0330
R	middle frontal gyrus	10	25	51	9		0.7039
R	middle frontal gyrus	6	30	7	54		0.1178
L	inferior frontal gyrus	45	−51	22	8		0.1846
L	inferior frontal gyrus **	13	−39	21	4		**0.0035**
R	inferior frontal gyrus **	13	37	21	9		**0.0011**
L	insula, anterior	13	−33	3	13		0.0103

			Talairach Coordinates			p *	
	Region	**BA**	**x**	**y**	**z**	**PCC**	**ACC**
L	posterior cingulate	23	−2	−51	23		**3.5×10^{-5}**
L	lingual gyrus	18	−4	−83	−2		0.0184
L	caudate		−11	13	8		0.0899
R	caudate		14	17	7		0.1580
L	putamen		−20	10	8		0.0111
R	putamen **		23	11	6		**0.0008**
L	thalamus		−6	−12	10		0.2636

*Results of paired Student's t-tests between groups. Values in bold survived the FDR correction.

**Regions where connectivity is stronger in DS as compared to controls.

Table 2.

Correlation coefficients indicating the strength of connectivity to plasma measures and inflammatory cytokines. Inflammatory markers are separated by known function into general categories of anti-inflammatory, immunoregulatory/pleiotropic, and proinflammatory. L ITG = left inferior temporal gyrus (BA 20); L IFG = left inferior frontal gyrus (BA 47); L AG = left angular gyrus (BA 39); R AG = right angular gyrus (BA 39); R IFG = right inferior frontal gyrus (BA 47); L Thal = left thalamus.

	PCC		ACC			
	L ITG	**L IFG**	**L AG**	**R AG**	**R IFG**	**L Thal**
Plasma measures						
$A\beta_{1-40}$	−0.4407	0.5056	−0.0228	−0.4808	0.5877	−0.3996
$A\beta_{1-42}$	−0.1692	0.6601	−0.2640	−0.1287	0.0739	−0.1222
t-tau	0.2639	−0.2981	0.2786	**0.7543** ^	−0.2521	0.5998
sTREM2	−0.4488	0.5584	**0.7273** ^	0.3069	0.5316	0.2951
Anti-inflammatory						
IL-1RA	−0.3011	0.0072	**0.7973** ^	**0.8736** **	0.5588	**0.7832** ^
IL-4	−0.3359	0.3011	**0.8669** *	0.6065	0.0153	0.4260
IL-5	−0.1216	0.0416	**0.9176** **	**0.7884** ^	0.4586	0.7007
IL-10	−0.5929	0.5399	0.3920	0.2465	**0.7699** ^	0.2204
IL-13	−0.2727	0.0185	**0.7876** ^	**0.8847** **	0.5299	**0.7684** ^
FGF-2	**−0.8929** **	0.6782	0.4528	0.3241	0.5706	0.1540
G-CSF	**−0.7532** ^	0.7316	0.4852	0.2985	0.4806	0.1745
Immunoregulatory/pleiotropic						
IL-6	**−0.7950** ^	0.4694	0.3893	0.3949	**0.7272** ^	0.3125
IL-7	−0.7323	0.7126	0.4937	0.2468	0.4059	0.0726
IL-9	**−0.7331** ^	0.4465	0.4560	0.4782	**0.7557** ^	0.4138
TGF-α	−0.6786	0.4059	0.6090	0.6399	0.6141	0.5781
Fractalkine	**−0.8225** *	0.6028	0.5461	0.1712	0.5536	−0.0203
MDC	**−0.8211** *	0.7422	0.4021	0.0079	0.6274	−0.0965
Proinflammatory						
IL-1α	**−0.7565** ^	**0.7527** ^	0.4380	0.3076	0.3547	0.3406
IL-1β	**−0.9186** **	0.7185	0.4799	0.2941	0.5680	0.1495
IL-2	**−0.9099** **	**0.7618** ^	0.4365	0.2809	0.6189	0.1525
IL-3	−0.2813	0.4409	0.5634	0.4067	0.6749	0.3836
IL-8	−0.3876	0.1445	**0.7729** ^	**0.8508** **	0.5782	**0.7482** ^
IL-12P40	−0.6142	0.5935	0.6183	0.1941	0.6660	0.0481
IL-12P70	**−0.8873** **	0.6768	0.5002	0.3691	0.5291	0.2307
IL-15	−0.6925	0.5065	0.5495	0.4421	**0.8320** **	0.3643

	PCC		ACC			
	L ITG	**L IFG**	**L AG**	**R AG**	**R IFG**	**L Thal**
IL-17A	**−0.8625** *	**0.7467** ^	0.5084	0.1336	0.6179	0.0052
IP-10	0.0019	0.4710	0.0675	0.0834	−0.1380	0.2596
EFG	−0.3562	0.0827	0.6400	**0.7927** ^	0.5816	0.7113
Eotaxin	−0.3610	0.1563	**0.8798** **	**0.8629** **	0.5103	**0.7598** ^
Flt-3L	−0.7405	0.4912	0.5664	0.0353	0.5546	−0.1252
GM-CSF	**−0.8512** *	0.6368	0.5275	0.4564	0.6357	0.3246
IFNα2	−0.6770	**0.8109** ^	0.3986	0.1551	0.3274	0.0450
IFNγ	**−0.7952** ^	0.7035	0.6354	0.2982	0.5851	0.2055
GRO	−0.2525	0.5314	0.4650	0.2203	0.1693	0.0418
MCP-1	0.0016	0.1893	0.4054	0.1976	0.1012	0.4210
MCP-3	0.0545	−0.2921	**0.8378** *	**0.8233** ^	0.2977	0.6746
sCD40L	**−0.8590** *	**0.8155** *	0.5034	0.1757	0.5691	0.0927
MIP-1α	−0.5745	0.2939	0.6256	0.6646	0.6611	0.5877
MIP-1β	**−0.8329** *	0.7045	0.5512	0.3798	0.6436	0.3077
TNFα	**−0.7229** ^	0.6407	0.7035	0.2785	0.5069	0.1788
TNFβ	−0.1987	0.5280	0.7140	0.7459	0.0224	0.5345
VEGF	**−0.8790** **	0.7467	0.5232	0.2771	0.4802	0.1573

^ $p < 0.02$;

* $p < 0.005$;

** $p < 0.001$.

Values in bold survived the FDR correction.